

## Supporting Information

### Self-Standing Cellulose Nanofibers/ Poly(3,4-ethylenedioxythiophene):

### Poly (4-styrenesulfonate)/Ionic Liquid Actuators with Superior Performance

Naohiro Terasawa\*, Kinji Asaka

**Table S1:** Specific capacitance,  $C = C_1$ , divided by the weights of PEDOT:PSS ( $F g^{-1}$ ) in CNF/PEDOT:PSS/IL electrodes (applied triangular voltage:  $\pm 0.5$  V, sweep rate:  $1 \text{ mV s}^{-1}$ ).

IL	LB/ PEDOT			BB/ PEDOT		
	50	200	200	50	200	200
EMI[BF <sub>4</sub> ]	24.0			24.1		
EMI[CF <sub>3</sub> SO <sub>3</sub> ]	26.5			26.3		

**Table S2:** Electrical conductivity ( $S \text{ cm}^{-1}$ ) of CNF/PEDOT:PSS/IL electrodes.

IL	LB/ PEDOT			BB/ PEDOT		
	50	200	200	50	200	200
EMI[BF <sub>4</sub> ]	6.3			5.0		
EMI[CF <sub>3</sub> SO <sub>3</sub> ]	4.8			4.8		

**Table S3:** Maximum strain (%) of CNF/PEDOT:PSS/IL (50/100/200) electrodes.

<b>IL</b>	<b>LB/ PEDOT</b>	<b>BB/ PEDOT</b>
<b>EMI[BF<sub>4</sub>]</b>	<b>0.45</b>	<b>0.72</b>
<b>EMI[CF<sub>3</sub>SO<sub>3</sub>]</b>	<b>0.39</b>	<b>0.46</b>

**Table S4:** Maximum strain (%) of CNF/PEDOT:PSS/IL (50/200/200) and PEDOT:PSS/IL electrodes.

<b>IL</b>	<b>LB/PEDOT</b>	<b>BB/ PEDOT</b>	<b>PEDOT</b>
<b>EMI[BF<sub>4</sub>]</b>	<b>0.74</b>	<b>1.04</b>	<b>0.26*</b>
<b>EMI[CF<sub>3</sub>SO<sub>3</sub>]</b>	<b>0.64</b>	<b>0.78</b>	<b>0.48*</b>

\* Ref. [33]

**Table S5** Maximum generated stress values (MPa) of the (50/200/200) and PEDOT:PSS/IL electrodes.

--	--	--	--

IL	LB/PEDOT	BB/PEDOT	PEDOT
EMI[BF <sub>4</sub> ]	1.02	1.41	0.35*
EMI[CF <sub>3</sub> SO <sub>3</sub> ]	0.90	1.22	0.49*

\* Ref. [33]

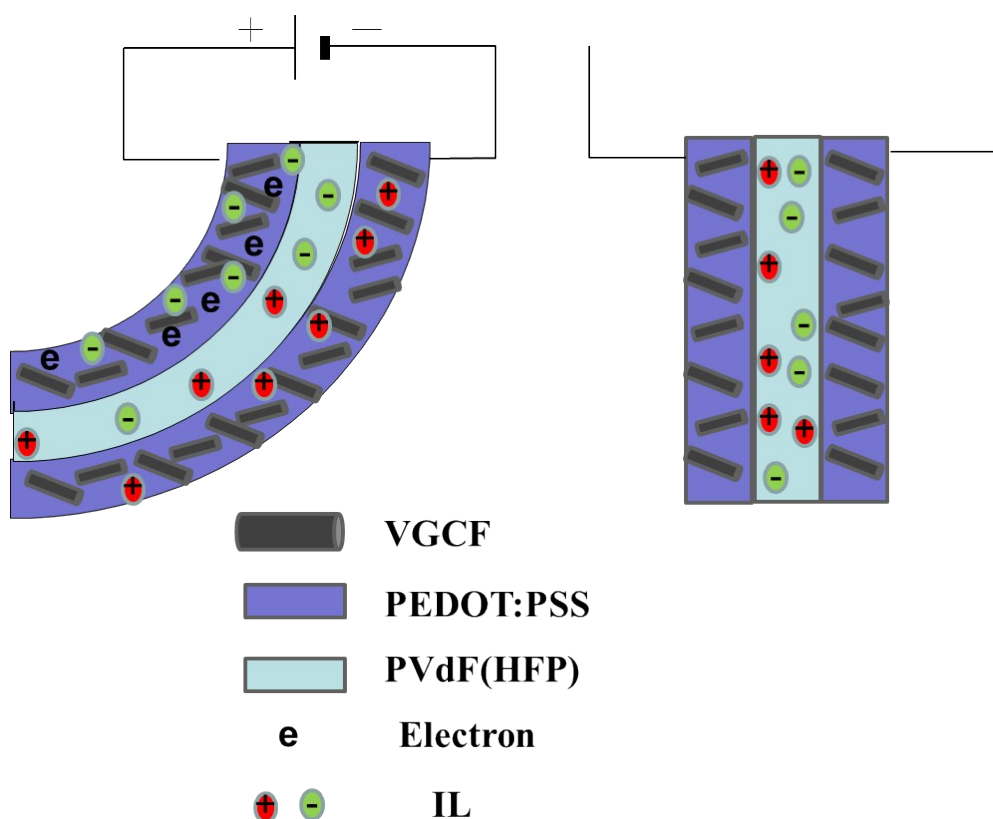


**Figure S1:** Schematic of the response model used for the PEDOT:PSS/VGCF/IL actuators.

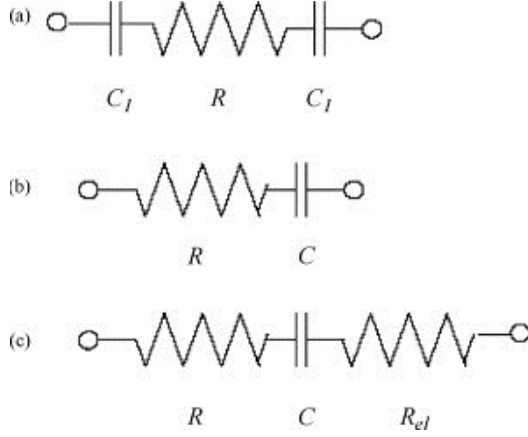


**Figure S2:** Three equivalent circuit models for the CNF actuator, where  $C_1$  and  $C$  are specific resistances (with  $C = C_1/2$ ),  $R$  is the ionic resistance, and  $R_{el}$  is the electrode resistance.

**Figure S2** presents equivalent circuit models for CNF/PEDOT:PSS/IL, actuators. The model in **Figure S2(a)** consists of the specific capacitance  $C_1$  between the CNF/PEDOT:PSS/IL electrode and the electrolyte layer; and the resistance,  $R$ , associated with the electrolyte layer. **Figure S2(b)** shows a more simplified model in which the two  $C_1$  capacitances are replaced by a single capacitance  $C (= C_1/2)$ . When a triangular voltage with an amplitude of  $\pm A$  and frequency of  $f$  is applied to the equivalent circuit shown in **Figure S2(b)**, the maximum accumulated charge  $Q(f)$  can be expressed as follows [S1]:

$$Q(f)/Q_0 = 1 - 4CRf(1 - \exp(-1/4CRf)), \quad (\text{S1})$$

where  $Q_0$  is the accumulated charge at the low-frequency limit. If the strain  $\varepsilon$  in the electrode layer is proportional to the accumulated charge, then it can be calculated as follows:

$$\varepsilon = \varepsilon_0 Q(f) / Q_0, \quad (\text{S2})$$

where  $\varepsilon_0$  is the strain at the low-frequency limit.

When conduction is considered in the electrode layer, it is necessary to account for the electrode resistance in the equivalent circuit. If the electrode resistance is treated explicitly, then the equivalent circuit should be treated as a distributed transmission line [S2]. Here, we assumed that the electrode resistance consists of a resistance element,  $R_{el}$ , as shown in **Figure S2(c)**. Thus,  $R$  in Eq. (S1) can be replaced by  $R + R_{el}$ .

To evaluate the double-layer charging kinetic model, which accounts for the oxidization and reduction reactions of the PEDOT, the specific capacitances of the CNF/PEDOT:PSS/IL electrodes were measured along with the ionic resistance of the gel electrolyte layer. The frequency dependence of the strain was calculated using Equation (S1) and Equation (S2). **Figure S3** shows the frequency dependence of the measured strain values together with the simulation results for the BB/PEDOT:PSS/EMI[BF<sub>4</sub>] (50/200/200), actuators. Curve A was calculated using the model shown in **Figure S2(b)**, whereas **Table S6** lists the simulation parameters. Curve B was calculated using the model shown in **Figure S2(c)**, and the corresponding simulation parameters are listed in **Table S7**. **Figure S3** clearly shows that the frequency dependence of the strain is closely reproduced by Curve B. **Figure S3** further reveals that the frequency dependence of the strain is reproduced by the double-layer charging kinetic model when the electrode resistance is considered. Similar results were obtained for the LB/PEDOT:PSS/EMI[BF<sub>4</sub>] (50/200/200), CNF/PEDOT:PSS/EMI[CF<sub>3</sub>SO<sub>3</sub>] (50/200/200) and CNF/PEDOT:PSS/IL (50/100/200) actuators.

The strain values were fitted to the low-frequency limit, as shown in **Figure S3**, by choosing appropriate values for  $\varepsilon_0$  in Eq. (S2). These are listed in **Table S7**.

The results summarized in **Table S6** and **Table S7** should be considered with respect to both the kinetic and static components to obtain an actuator with optimal performance. From a kinetic viewpoint, the most important consideration is that the frequency dependence of the strain is determined by electrochemical charging, as shown in **Figure S3**. Thus, obtaining good fits generally requires taking the electrode resistance into account, and the responses of the CNF/PEDOT:PSS/IL actuators can be improved by fabricating electrodes with higher conductivities.

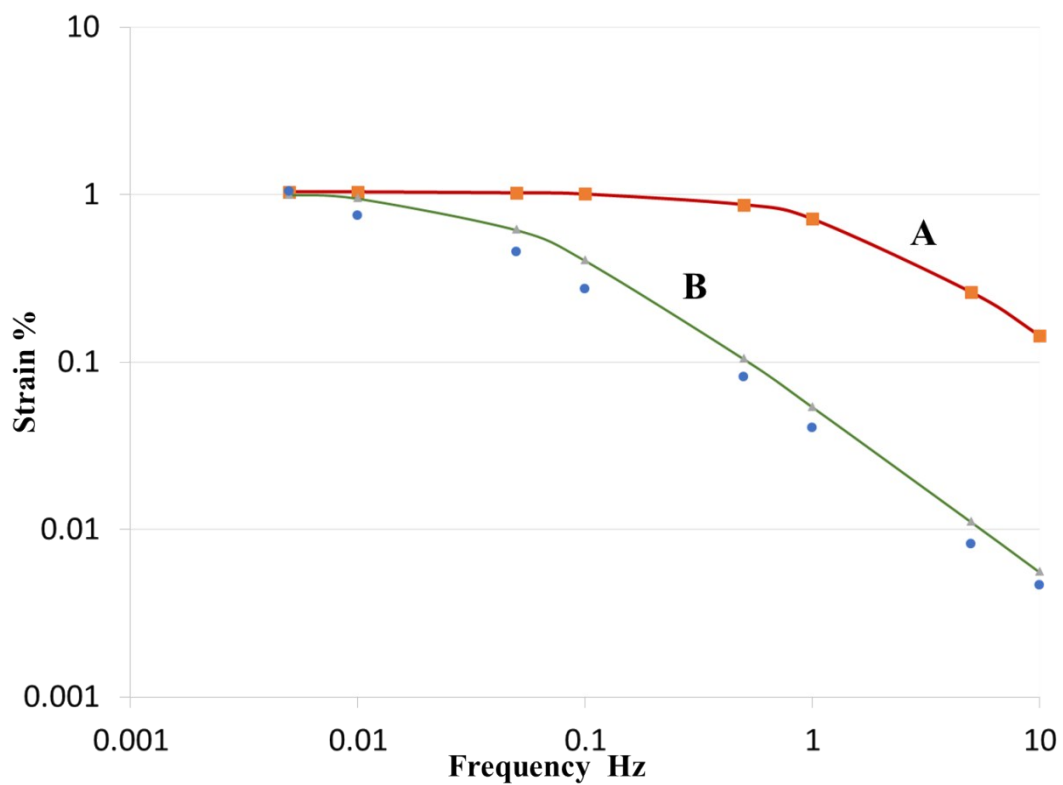


**Figure S3:** Measured (blue dots and orange rectangular symbols) and simulated (green and red curves) data showing the frequency dependence of the strain for a BB/PEDOT:PSS/EMI[BF<sub>4</sub>] (50/200/200) device. Curves A and B were calculated using the equivalent circuits in **Figures S2(b)** and **S2(c)**, respectively.

**Table S6:** Simulation parameters for the CNF/PEDOT:PSS/IL (50/200/200) model that ignores electrode resistance.

CNF/IL	$C_{PEDOT}$ (F g <sup>-1</sup> )	$C$ (F cm <sup>-2</sup> )	$\kappa$ (mS cm <sup>-1</sup> ) <sup>a)</sup>	$R$ ( $\Omega$ cm <sup>2</sup> )	$\varepsilon_0$ (%)	$CR$ (s)
LB/[BF <sub>4</sub> ]	24.0	0.2803	2.8	0.714	0.74	0.2001
BB/[BF <sub>4</sub> ]	24.1	0.1807	2.8	0.714	1.04	0.1290
LB/[CF <sub>3</sub> SO <sub>3</sub> ]	26.5	0.2657	4.4	0.455	0.64	0.1209
BB/[CF <sub>3</sub> SO <sub>3</sub> ]	26.3	0.2488	4.4	0.455	0.78	0.1132

<sup>a)</sup> ref. [S3]

**Table S7:** Simulation parameters for the CNF/PEDOT:PSS/IL (50/200/200) model that considers electrode resistance.

IL	$C$ (F cm <sup>-2</sup> )	$R_{el}$ ( $\Omega$ cm <sup>2</sup> )	$R+R_{el}$ ( $\Omega$ cm <sup>2</sup> )	$C(R+R_{el})$ (s)
LB/[BF <sub>4</sub> ]	0.2803	10.6	11.3	3.17
BB/[BF <sub>4</sub> ]	0.1807	12.5	13.2	2.39
LB/[CF <sub>3</sub> SO <sub>3</sub> ]	0.2657	13.4	13.9	3.69
BB/[CF <sub>3</sub> SO <sub>3</sub> ]	0.2488	13.9	14.4	3.58

$R_{el}$  = area of the electrode film (cm<sup>2</sup>)/[electrical conductivity (S cm<sup>-1</sup>) × thickness of the electrode film (cm)] [S1].

## References

- [S1] I. Takeuchi, K. Asaka, K. Kiyohara, T. Sugino, K. Mukai, T. Fukushima and T. Aida, *Electrochim. Acta*, 2009, **53**, 1762-1768.
- [S2] K. Takagi, Y Nakabo, Z.-W. Luo and K. Asaka, *Proceedings of the SPIE, Electroactive Polymer Actuator and Devices (EAPAD)*, 2007, **6524**, 652416-1-652416-8.
- [S3] N. Terasawa, I. Takeuchi and H. Matsumoto, *Sens. Actuators B*, 2009, **139**, 624-630.